PROCEEDINGS, 48th Workshop on Geothermal Reservoir Engineering
Stanford University, Stanford, California, February 6-8, 2023
SGP-TR-224

New Maps of Conductive Heat Flow in the Great Basin, USA: Separating Conductive and Convective Influences

Jacob DEANGELO[1], Erick R. BURNS[2], Emilie GENTRY[3], Joseph F. BATIR[3], Cary R. LINDSEY[2], Stanley P. MORDENSKY[2].

[1]U.S. Geological Survey, Moffett Field, Mountain View, CA, USA

[2]U.S. Geological Survey, 2130 SW 5th Ave, Portland OR 97201, USA

[3]Petrolern, 1048 Arbor Trace NE, Brookhaven, GA 30319, USA

jdeangelo@usgs.gov

Keywords: Conductive heat flow, convective heat flow, Great Basin, heat flow map, hydrothermal, quality code, thermal gradient wells, trend, uncertainty

ABSTRACT

Geothermal well data from Southern Methodist University and the U.S. Geological Survey (USGS) were used to create maps of estimated background conductive heat flow across the Great Basin region of the western United States. These heat flow maps were generated as part of the USGS hydrothermal and Enhanced Geothermal Systems resource assessment process, and the creation process seeks to remove the influence of hydrothermal convection from the predictions of the background conductive heat flow. The heat flow maps were constructed using a custom-developed iterative process using weighted regression, in which convectively influenced outliers were de-emphasized by assigning lower weights to measurements with heat flow values further from the estimated local trend (e.g., local convective influence). The local linear weighted regression algorithm is two-dimensional locally estimated scatterplot smoothing where smoothness was controlled by varying the number of nearby wells used for each local interpolation.

Three maps resulting from conductive heat flow models are detailed in this paper, highlighting the influence of measurement confidence. The three maps use either: measurements from all wells with equal weight (no confidence weights), or one of two different published categorization methods to de-emphasize low-quality measurements; one categorization method graded thermal gradient quality, the other categorization method graded thermal conductivity quality. Each map is an estimate of background conductive heat flow as a function of reported data quality, and a point coverage is also provided for all wells in the compiled dataset. The point coverage includes an important new attribute for geothermal wells: the residual, which can be interpreted as the departure of a well from the estimated background heat flow conditions, and the value of the residual may be useful in identifying the influence of fluids (hydrothermal or groundwater) on conductive heat flow. Of the three maps presented, the map that de-emphasized the impact of wells with low-quality thermal gradient measurements appears to perform best because it did not incorporate many of the wells in the Snake River Plain that do not penetrate the aquifer and are therefore very unlikely to reflect true conductive conditions.

1. INTRODUCTION

Crustal heat flow occurs via both conduction and convection. The effects of the interplay between conductive and convective heat flow can be difficult to deconvolve because of their interdependence (e.g., the upward convection of hot water causes locally enhanced conductive heat flow). When attempting to model regional conductive heat flow from well measurements, two challenges become distinct. These challenges are: 1) hydrothermal systems (i.e., large convective disturbances) are sometimes sampled very densely when compared with the regional coverage of heat flow measurements; and 2) heat flow measurements from wells can be exceedingly large (> 20,000 mW/m² in Yellowstone [SMU, 2021]) when compared to the anticipated background conductive heat flow of active tectonic areas (70-80 mW/m²; Pollack et al., 1993). In this study, we present three conductive heat flow maps and supporting information for the region of the Great Basin in the United States (Figure 1). The three maps use either: measurements from all wells with equal weight (no confidence weights), or one of two different published categorization methods to de-emphasize low-quality measurements; one categorization method graded thermal gradient quality, the other categorization method graded thermal conductivity quality. Each of the new data products summarized herein consists of a background heat flow map and the complementary residuals (i.e., the difference between heat flow measured at a well and the background heat flow estimate). The background heat flow maps show regional patterns of conductive heat flow, and patterns of large residuals are generally associated with localized convective flow of hydrothermal fluids (e.g., convective flow) or possibly groundwater (e.g., advective flow).

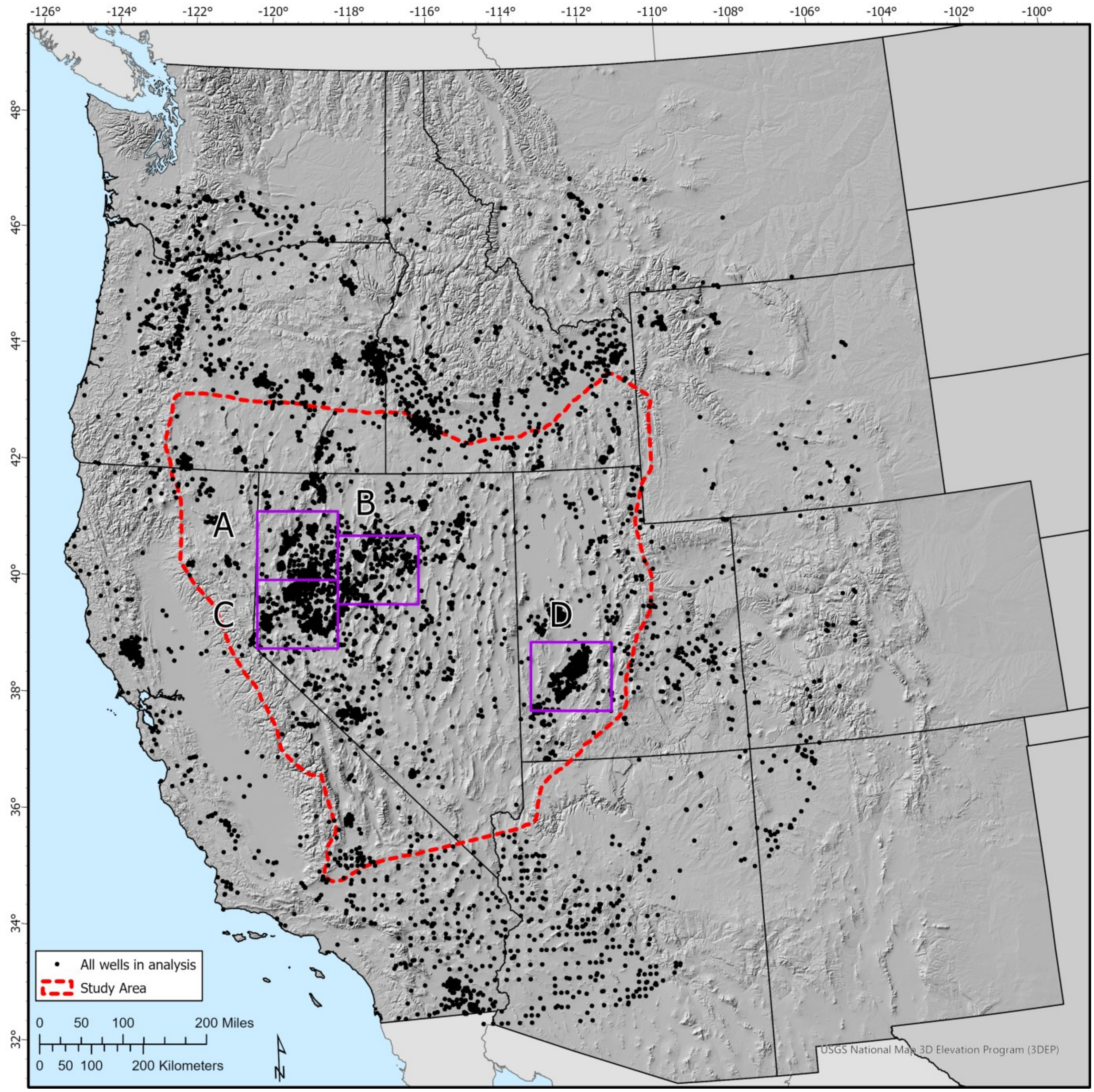

Figure 1: Overview map showing locations of well data used in the analysis, the footprint of heat flow maps (study area) in red, and purple boxes A, B, C, and D showing the extent of local-area maps presented in Figure 8. Hillshade from USGS 3D Elevation Program (U.S. Geological Survey, 2019).

2. METHODS

Heat flow maps were constructed using trend models that match the heat flow measurements that represent the broad pattern of background conductive heat flow across the Great Basin. Because the two challenges imparted by sampling bias and areas of convection-dominated measurements can bias a trend model, we systematically remove the influence of well data that is most likely to be strongly influenced by convection (DeAngelo et al., 2022). Wells that were removed or strongly de-emphasized during trend modeling are included in the associated published residual datasets, so future use of heat flow maps and residuals together ensure that no information is lost.

Three sets of maps with associated residuals are included in a U.S. Geological Survey (USGS) data release (DeAngelo et al., 2022) allowing comparison of three confidence weighting strategies: all wells with equal weight (no confidence weights) and two different reduced weighting schemes for wells with low-quality measurements. Low-quality weights ensure that higher-quality well data are emphasized. Low-quality well data weights were comparatively small (≤ 0.01), but never set to zero, allowing trend models to match these data if no high-quality data are nearby. The three map/residuals sets are:

1) Background heat flow assuming all wells have equal weight (no confidence weights).

2) Background heat flow, strongly de-emphasizing measurements with thermal gradient values judged to be of low quality by subject-matter experts (SMU, 2021).

3) Background heat flow, strongly de-emphasizing measurements with thermal conductivity values judged to be of low quality by subject-matter experts, translating to uncertainty in heat flow estimates (University of Nevada, Reno, 2022).

The workflow for map construction is as follows:

1) Compile available datasets, including available qualifiers that are related to heat flow measurement quality. Select relevant data for use in analysis: selecting which heat flow measurement best represents a well, removing wells that have no heat flow data or are very distant (> 400 km) from the study area.

2) Reduce the density of measurements in the vicinity of hydrothermal systems by removing measurements that are strongly convectively influenced and retaining measurements that are representative of background conductive heat flow.

    2.1) Compute geostatistical cell-based declustering weights (Pyrcz et al., 2021) to identify areas of dense sampling (i.e., areas near hydrothermal systems).

    2.2) Construct an overly smooth trend model to identify which heat flow measurements in densely sampled areas are most similar to background heat flow (using the trend modeling summarized in Step 3).

    2.3) Remove wells from the densely sampled areas (from Step 2.1) that have highest residuals (from Step 2.2). This ensures that only background heat flow measurements from dense areas are used for constructing the regional conductive heat flow patterns. [*Note*: Wells removed in this step are removed from Step 3 interpolation, but still have a residual calculated for them (see Step 5).]

3) After removing dense data in hydrothermal areas, we produce regional trend maps using an iterative procedure that de-emphasizes outliers and emphasizes data that support a smooth background heat flow trend surface. The final surface generally has the following properties for the emphasized data:

    3.1) There are many datapoints with small residuals in nearly all areas of the map that were sampled. If residuals are larger, there should be no large trends in positive or negative residuals (i.e., the residuals are random, indicating a good fit on average).

    3.2) There are no large numerical artifacts in areas with no data (e.g., a trend does not create a high or low heat flow estimate that is not supported by measurement data).

4) Step 3 above is repeated for each confidence weight strategy, which means that low quality data are de-emphasized prior to and during iteration, ensuring these data are far less important on resulting maps (weight ≤ 0.01).

5) All heat flow measurements (i.e., emphasized data, de-emphasized data, and removed data) have a calculated residual associated with each heat flow map.

Details for these steps are given in the subsequent sections below.

2.1 Data Compilation

The Southern Methodist University (SMU) data were used as the foundational dataset (SMU, 2021). Some wells in the SMU data have multiple entries reflecting multiple depth sections of the same well. The SMU data were supplemented with additional data from the USGS (Sass et al., 2005). The SMU data have a field for 'heat flow' of a well and a field for 'corrected heat flow;' the latter is higher quality. Therefore, a new field 'hf_meas' containing the best heat flow estimate for interpolation was generated by using the 'corrected heat flow' if that estimate was available on a per entry (i.e., row) basis, otherwise the 'heat flow' value was used. To ensure proper distance computation during interpolation, new coordinates (in meters) were established using a custom Albers Equal Area Conic projection centered at -117° using the NAD83 datum. These coordinates (i.e., x and y, corresponding to easting and northing), along with the hf_meas value (i.e., z) became the x, y, and z values required as inputs to the locally estimated scatterplot smoothing (LOESS) trend modeling function (Cleveland et al., 1992; LOESS, 2022) used to construct the background heat flow maps.

The combined SMU and USGS data contained many records, or entries, that were not used in the analysis. Wells with multiple depth intervals had all entries removed aside from the entry SMU identified as having the 'highest quality depth data' and were therefore most likely to represent background conductive conditions. SMU entries that were duplicates of USGS entries were removed. Entries with no data for heat flow were removed. Wells that were more than 400 km from the study area were removed, as were wells that were either in the Pacific Ocean or had no location information. This reduced the total number of entries in the combined SMU and USGS database from 15,840 entries to 7,279 entries. Each of these 7,279 heat flow measurements came from an individual well.

The 7,279 entries used in the present analysis were not uniformly distributed across the study area. The history of geothermal exploration resulted in a bias where wells were often preferentially located in places that people thought were likely to host a hydrothermal system.

This resulted in groups of wells existing near known or suspected hydrothermal systems, many of which were likely to be influenced by local convection.

2.2 Confidence Weighting

Two of the three models for heat flow in this study weight well values depending on their categorized confidence in the thermal gradient measurement and in the reported thermal conductivity. Heat flow is calculated by multiplying the measured thermal gradient by reported thermal conductivity of the measured interval. Because errors in heat flow estimates depend on both properties, every heat flow estimate used herein was examined using quality categories that represent both thermal gradient and thermal conductivity quality. Confidence weights were implemented by using an expert-defined weight multiplier designed to lower the influence of low-confidence wells during trend modeling (Tables 1 and 2; Figure 2). This strategy causes the trend model to fit higher confidence data preferentially when high- and low-quality data are near each other.

The SMU database calls the thermal gradient quality the ‘quality code’, assigning a letter corresponding to relative quality of temperature profiles used for computing heat flow estimates (Table 1; Figure 2A). A portion of the full SMU dataset (examining only part of the Great Basin [4,138 of the 7,279 wells]) has been amended using published data to indicate whether thermal conductivity was measured, estimated, or of unknown origin, giving an implicit confidence in the corresponding values (Table 2, University of Nevada, Reno, 2022; Figure 2B). ‘A’ quality and ‘X’ quality designations in Table 2 were inherited from the ‘A’ & ‘X’ in Table 1. Points identified as ‘not labeled’ refer to the remainder of the 7,279 wells.

Table 1: SMU thermal gradient quality code information (SMU, 2021) and associated confidence weighting.

Quality Code Category	Definition (SMU, 2021)	Confidence Weighting	Count
A	High Quality Data: Deeper than 100 meters with at least a 50-meter linear gradient	1.0	1,241
B	Medium Quality Data: Deeper than 50 meters with gradient corrections applied	1.0	1,435
C	Poor Quality Data: Shallow or has some isothermal section	1.0	1,311
D	Use for background information but not mapping	0.01	422
G	Geothermal System: too high a value for regional maps	1.0	2,707
X	Data accuracy low but want site recorded	0.01	163

Table 2: Thermal conductivity quality code names (University of Nevada, Reno, 2022) and associated confidence weighting.

Thermal Conductivity Category	Confidence Weighting	Count
‘A’ quality	1.0	1,241
Known measured	1.0	1,435
Assumed measured	1.0	1,311
Unmeasured	0.01	422
‘X’ quality	0.01	2,707
Not labeled	1.0	163

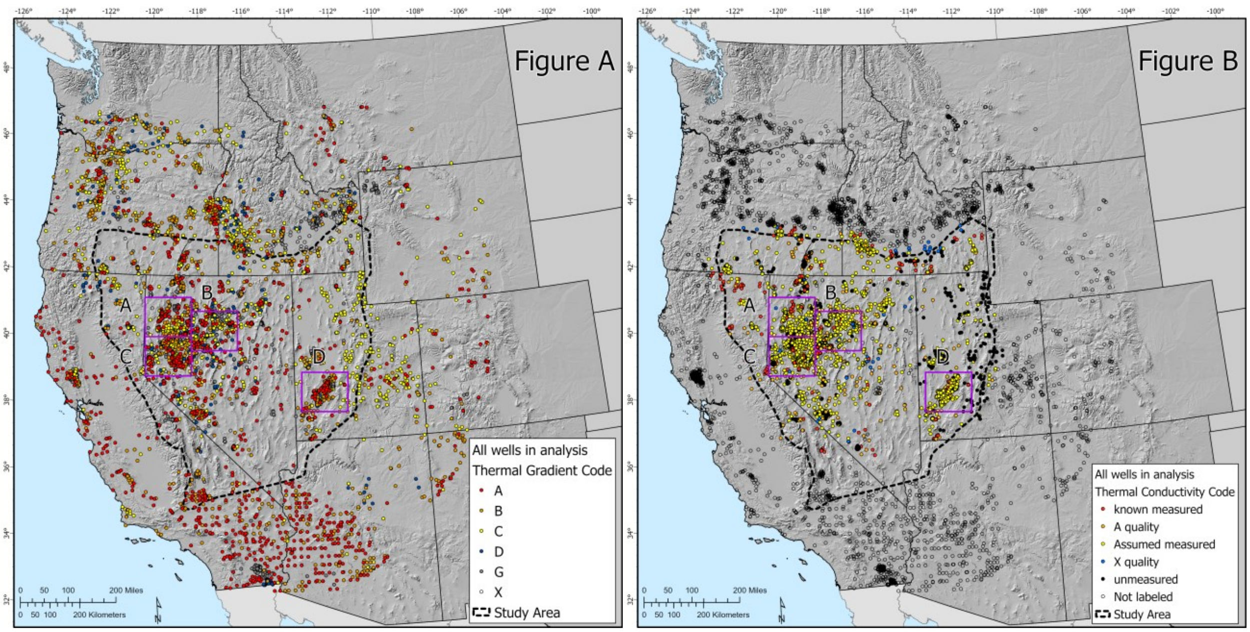

Figure 2: Maps showing quality codes assigned to wells from published data for: A) thermal gradient quality and B) thermal conductivity quality. The footprint of heat flow maps (study area) is shown with the black dashed line, and purple boxes A, B, C, and D show the extent of local-area maps presented in Figure 8. Hillshade from USGS 3D Elevation Program (U.S. Geological Survey, 2019).

Wells with the quality code of ‘A’ or ‘B’ were identified as being the highest quality and generally having reliable heat flow estimates. Wells with quality codes of ‘X’ and ‘D’ were viewed as likely to be of poor quality. The other designations of ‘C’ and ‘G’ were assumed to be of unknown quality. The SMU database assigned the ‘G’ designation to wells that were believed by the authors to likely reflect convective conditions in an active hydrothermal system. Reviewing the distribution of these ‘G’ wells revealed that many of these ‘G’ wells are likely to be convective, having relatively high values of heat flow (often over 200 mW/m²), but many were not; many of the ‘G’ wells had a wide range of values, some of which may be representative of conductive heat flow. Because the ‘G’ designation appeared to contain an unknown mixture of conductive and convective wells, all wells with a ‘G’ designation were used in modeling. Of these wells, those that appear strongly influenced by convection were removed or strongly de-emphasized by the procedures described in Sections 2.4 and 2.5. USGS wells were all assumed to be of high quality, so they were assigned ‘A’ designations for all entries, unless it was suspected the well is reflecting convective conditions, in which case a ‘G’ was assigned. It is important to note, there could be data designated as ‘G’, ‘C’, ‘D’, or ‘X’ that could be high quality data; however, re-examination of individual sites’ temperature data was not performed as part of this work. A review of approaches in characterizing heat flow data quality (Richards et al., 2012) describes several approaches that all conclude heat flow values are likely to contain substantial uncertainties arising from uncertainties in calculating both the thermal gradient and thermal conductivity. The highest quality SMU entries (‘A’ designation) were estimated to have uncertainties up to 10%, ‘B’ entries were estimated to have uncertainty up to 20% (Richards, 2013).

The SMU quality codes served two purposes in each of the two weighted models. First, wells with the designations ‘A’ and ‘B’ were not removed during preprocessing, which sought to remove wells with convective influence in densely sampled areas (described in ‘Removing Convective Wells in Densely Sampled Areas’ Section 2.5). Second, the SMU quality codes were used to de-emphasize (weight = 0.01) low-quality wells (‘X’ & ‘D’ wells) from the analysis. This resulted in an alternate heat flow map (and associated residuals) made with the intent of checking whether these low-quality wells had a substantial impact on predictions.

A similar workflow was undertaken using the thermal conductivity quality designations. An alternate heat flow model was produced that strongly de-emphasized (weight = 0.01) entries of low quality, specifically entries known to have unmeasured thermal conductivity and wells that were assumed to have poor thermal conductivity quality because they received an ‘X’ SMU quality code designation. This also resulted in an alternate heat flow map and associated residuals.

2.3 Interpolation Algorithm

A trend modeling algorithm, two-dimensional (2D) LOESS (LOESS, 2022), constructed the background heat flow maps. As used herein, the LOESS algorithm uses a fixed number of points (controlled by the ‘span’ parameter as a fraction of total points from 0 to 1) to estimate heat flow using local linear regression (parameter ‘degree’ equal to 1) at each location in an analysis, giving higher weights to nearby input points using a tricube weight function. Using more points (a higher span) results in a smoother map surface, while using fewer points (a lower span) results in a map with greater local-scale variation. Span is computed in terms of ‘number of points used for interpolation’ as [span = number of points desired/total number of points].

2.4 Iterative De-emphasis of Convectively Dominated Measurements

LOESS was used iteratively to de-emphasize convectively influenced measurements by computing weights in each iteration that progressively emphasize background conductive heat flow measurements and de-emphasize convectively dominated measurements. Input data points can be assigned weights in LOESS from 0 to 1 to emphasize or de-emphasize data points. Using this weighting ability, an iterative approach was developed where wells that had a heat flow value substantially above or below the estimated local trend would be assigned a lower weight in the next model iteration. To accomplish this, a custom function (Equation 1, Figure 3) was developed to relate the magnitude of a well's departure from the estimated heat flow at that location, or residual, to the weight it would be assigned for the next iteration. With each iteration, this process gradually lowered the influence of wells with heat flow far from the local trend, until no further changes were observed in the next iteration's model outputs and iterations ceased.

$$\lambda = 1 \qquad when\ |\alpha| \leq T, \tag{1 - a}$$

$$\lambda = -1 * \left(\frac{ln(W)}{R-T}\right) \qquad when\ |\alpha| > T, \tag{2 - b}$$

where λ = weight, α = residual, T = threshold of residual for well to get full weight, R = residual value, and W = weight at R.

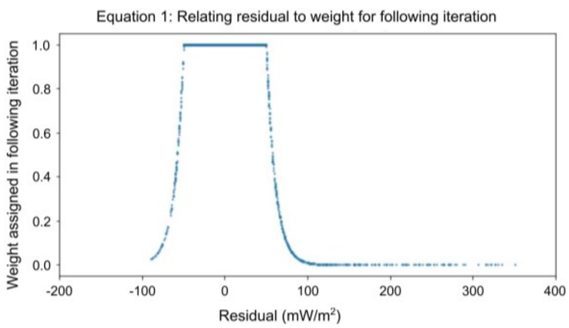

Figure 3: Custom function (Equation 1) relating the magnitude of a well's departure from the estimated heat flow at that location, or residual, to the weight that well would be assigned for the next iteration.

This iterative LOESS-based approach was developed to gradually remove the influence of wells that do not represent background conductive conditions. With each model iteration, convective wells were given lower weights, so the subsequent model predicted lower values at those and nearby well locations, causing nearby wells that may also be convective to be given lower weights. This process repeated until no additional wells varied far (beyond T) from running local estimates and were therefore likely to reflect background conductive conditions.

The following workflow was employed to assign weights in the iterative processing:

1) Assign weights to all measurements. For the first iteration, each weight = 1.0. For subsequent iterations, weights are assigned based on magnitude of residuals (see Equation 1).

2) Apply confidence multipliers to weights to de-emphasize measurements deemed to be of low-quality (Tables 1 and 2).

3) Run LOESS to create a heat flow map.

4) Compute and examine residuals. Have the residuals changed since the prior iteration?

    a. If YES, then iterate by going to step 1 and computing new weights.

    b. If NO, then stop iteration.

This process was repeated until new estimates no longer differed from the previous iteration. The final model was used to estimate values at all well locations and all cell centers in the study area on a 250 m² grid.

2.5 Removing Convective Wells in Densely Sampled Areas

'Span' determines how many points are used for the local linear regression, therefore densely sampled areas introduced problems to the interpolation because a very small search radius is required to find the chosen number of points in dense areas (e.g., typically densely sampled valleys with hydrothermal systems). This forces LOESS to increasingly try to replicate local convective features when span is made smaller and smaller, resulting in modeling artifacts associated with trends in the data on the margin of convective systems. Because the purpose is to construct a background heat flow map, prior to the iteration described in Section 2.4, measurements in densely sampled areas are thinned to retain only measurements that are most consistent with regional conductive heat flow (i.e., wells in densely sampled areas that are strongly influenced by convection are removed for subsequent interpolations).

Two criteria were used to remove convectively influenced measurements in densely sampled areas prior to running the iterative modeling process (Section 2.4). First, a well had to be located in a 'densely sampled' area. Declustering weights (Pyrcz et al., 2021) were calculated for the 7,279 entries using the cell-based method. These declustering weights are a quantitative measure of how densely sampled the area was from which the well came (i.e., low declustering weights correspond to many nearby measurements). In addition to low declustering weight (chosen to be < 1.5 based on a peak of low values in the histogram of weights), for a well to be removed from the analysis, the well also needed to have an anomalously high or low heat flow compared with local conditions (residual magnitude > 15 mW/m²). To estimate local conditions, a very generalized, smooth model (800 points in span) was generated using the iterative approach, producing a map depicting very broad low-frequency variations in heat flow and did not contain any local-scale variations or substantial modeling artifacts.

Entries with residuals greater than ± 15 mW/m² in densely sampled areas (declustering weight < 1.5) were removed from the analysis unless they were deemed to be high quality measurements (defined as having a quality code of either 'A' or 'B'). Active tectonic areas are estimated to have an average heat flow around 75 mW/m², described as being between 70 – 80 mW/m² by Pollack et al. (1993). Richards (2013) estimates that even relatively high-quality geothermal wells can have errors up to 20%. Twenty percent of 75 mW/m² is 15 mW/m². Given the likelihood that any well could vary ± 15 mW/m² or more due solely to errors or uncertainties, this 15 mW/m² cutoff was used to remove wells from densely sampled areas.

3. RESULTS

3.1 Selected Fitting Parameters

Decisions were made about which values to choose in the different steps of the present analysis. This included decisions about:

1) How to choose parameters to remove non-representative well data in densely sampled areas where high sample density creates bias (see Section 2.5).

    a. A range of spans were considered to see which models best retain background wells and best remove convectively influenced wells with thermal gradient quality codes other than 'A' or 'B' in areas with declustering weights < 1.5 (i.e., high measurement density areas) using the residual magnitude threshold of ±15 mW/m² (see Section 2.5). The models using spans in the range of 700 – 1,000 points all produced very similar maps with background wells consistently having residual magnitudes typically < 15 mW/m². Convectively influenced measurements in densely sampled areas were removed from subsequent trend modeling using a span value of 800 points.

2) How to choose the parameter values for iterative weight computation (Equation 1) and subsequent interpolation to de-emphasize convectively influenced wells (Section 2.4).

    a. Equation 1 (example shown in Fig. 3) relates the residual of a well from any trend map iteration to the weight it will be assigned in the subsequent model iteration. The variable T in Equation 1 depicts how large in magnitude a residual can get before being de-emphasized (i.e., controls width of flat region with weight = 1 in Fig. 3), allowing for the possibility of randomly distributed errors or minor variations in trend with no penalty for use of the measurement in trend modeling. A value of $T = 50$ was chosen so that measurements with residuals of ± 50 mW/m² would receive a weight of 1.0 in the subsequent iteration (choosing a fairly large number ensures that wells have full weight unless measurement errors and convective influence are large [in this case, on the order of 50 mW/m²]). The variables R and W work together to control how fast weight decreases outside of the range of T. A value of $R = 100$ was chosen along with $W = 0.01$; ensuring that the weight falls rapidly to 0.01 (1%) at a residual magnitude of 100. Use of a natural log function in Equation 1 ensures that very large convectively dominated heat flow measurements (e.g., thousands of mW/m²) have minimal influence on weighted regression (i.e., weight multiplied by residual).

3) How to assign confidence weights for low-quality measurements.

    a. Low quality measurements were assigned a confidence weight multiplier of 0.01. This reduces the impact of a low-quality well to 1% of the weight value computed during each iteration, making a low-quality well have only a very small impact on the trend model (i.e., weights are guaranteed to be ≤ 0.01) in areas with higher confidence heat flow measurements nearby. If no high-quality data are nearby, then low-weight data control the shape of the trend surface.

3.2 Resulting Datasets: Heat Flow Maps and Complementary Residuals

Of the 7,279 wells examined, 4,216 wells in densely sampled areas had 'high' residuals (> 15 mW/m²), but 1,013 had a quality code of either 'A' or 'B', so were therefore not removed from subsequent trend modeling. For all three confidence weighting scenarios, the resulting total number of wells used for iterative heat flow map construction was 4,076.

A range of spans were considered during the iterative modeling process (20 - 400 points), and a span of 200 points was selected for published maps as having balanced effects of low residuals for background heat flow wells while minimizing numerical artifacts (e.g., spurious trends). Estimated background heat flow at wells with a weight equal to 1 (wells that are not de-emphasized for the trend) are on average correct (i.e., unbiased with the average residual near zero [= -0.51 mW/m²], and a symmetric distribution with standard deviation of 21.0 mW/m²). Figure 4 shows all residuals in the range ± 150 mW/m².

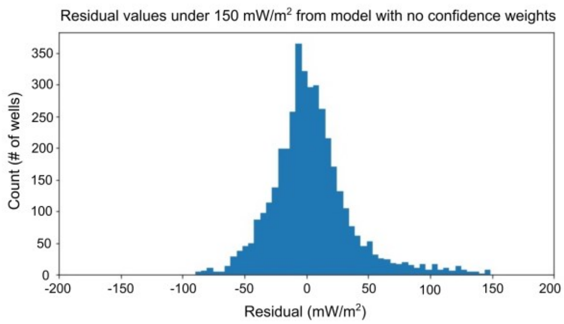

Figure 4: Histogram of residual values under 150 mW/m² from the model with no confidence weights following removal of wells from densely sampled areas.

The resulting heat flow maps (Figures 5, 6A, 6B) represent broad-scale trends of background conductive heat flow. The difference in heat flow maps resulting from using the two different confidence weights are shown in Figures 7A & 7B, with plots showing weighted results minus unweighted results. Because the interpolator is not an exact interpolator, measured heat flow values of individual wells used in the analysis were invariably different from estimated values at their locations; however, individual wells tended to be either close to the estimated value (i.e., had a low residual) and were likely reflective of background conductive conditions, or individual wells were very far from the locally estimated value (i.e., had a high residual) and are assumed to be likely convectively influenced or contain errors. Convectively influenced wells can often be observed in groups of large positive residuals (i.e., measured heat flow is larger than background) near known geothermal areas (Figure 8). The residual value calculated for each well represents the magnitude of a well's departure from the modeled background conductive heat flow conditions, therefore smaller residuals can reflect measurement error, and larger magnitude positive residuals more likely reflect hydrothermal upflow conditions.

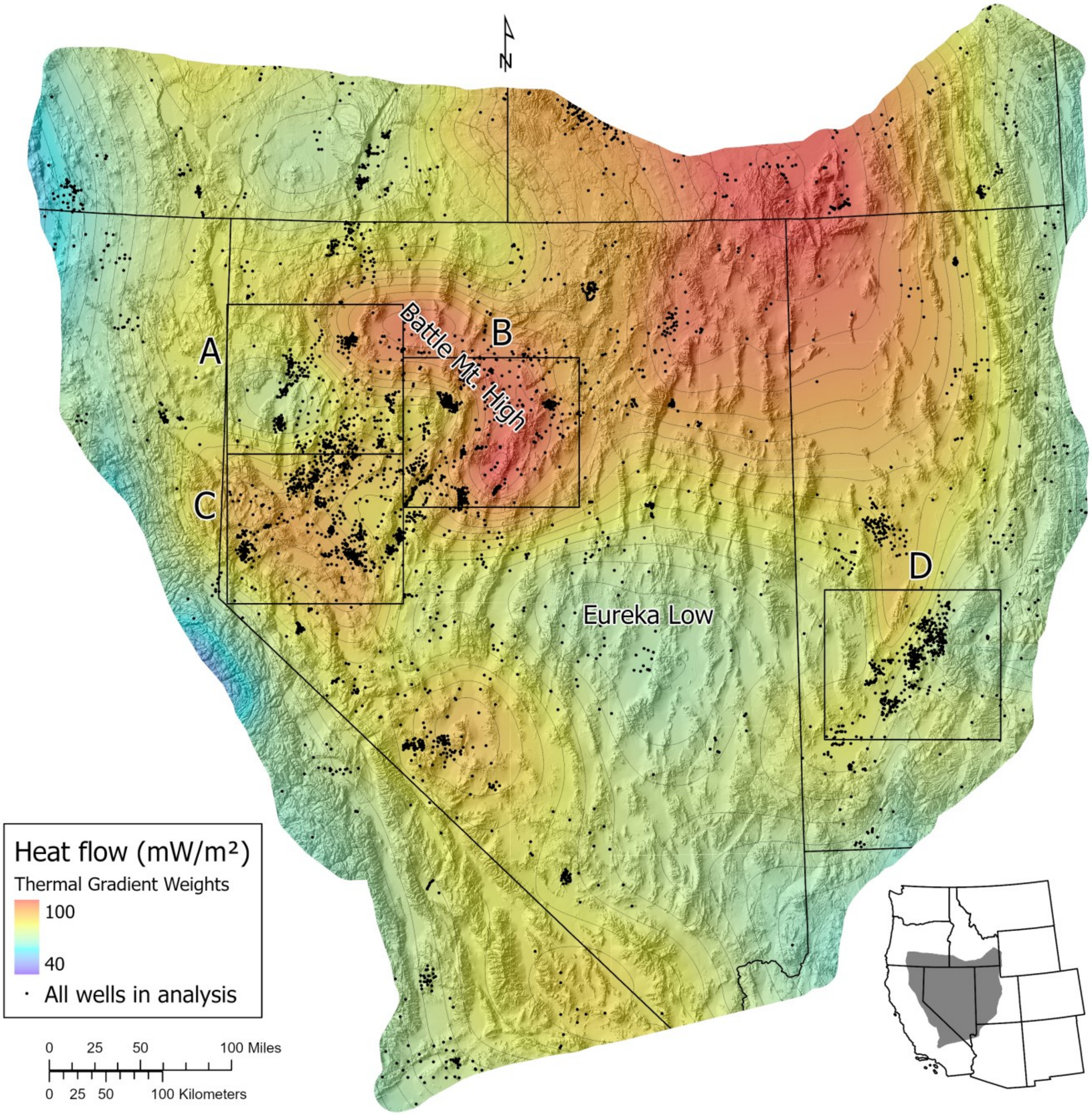

Figure 5: The preferred trend model of estimated background conductive heat flow map constructed using lower weights for wells that are deemed to have low-quality thermal gradient information (section 2.2; DeAngelo et al., 2022). Black boxes A, B, C, and D show the extent of local-area maps presented in Figure 8. Hillshade derived from USGS National Atlas (National Atlas of the United States, 2012).

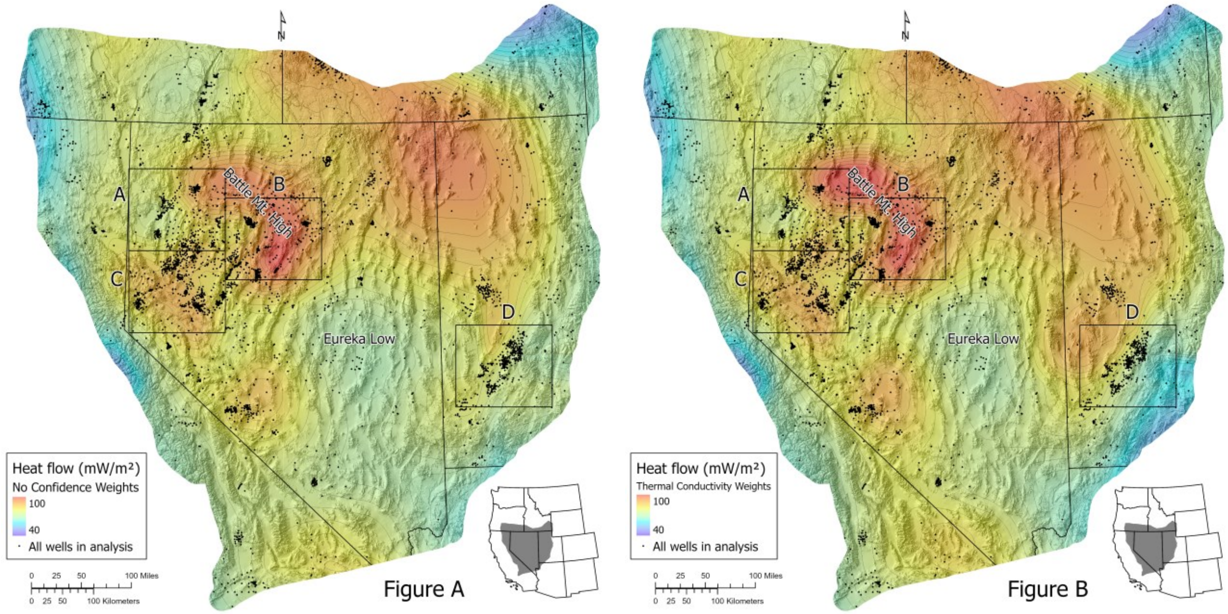

Figure 6: Estimated background conductive heat flow map using: A) no confidence weights (all wells used for iterative analysis start with equal weight =1); B) lower weights if well data are deemed to have low-quality thermal conductivity information (described in section 2.2; DeAngelo et al., 2022). Black boxes A, B, C, and D show the extent of local-area maps presented in Figure 8. Hillshade derived from USGS National Atlas (National Atlas of the United States, 2012).

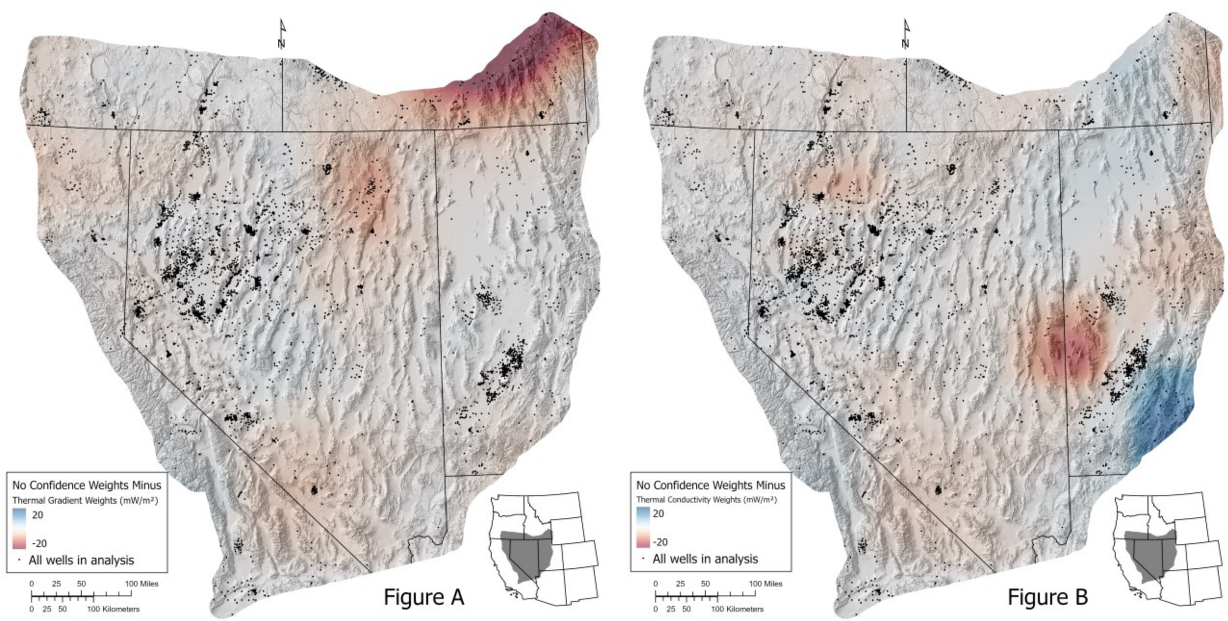

Figure 7: Differences in estimated heat flow resulting from adding confidence weights (i.e., heat flow estimated using no confidence weighting minus heat flow estimated using confidence weights) with A) quality codes weights and B) thermal gradient codes (DeAngelo et al., 2022). Hillshade derived from USGS National Atlas (National Atlas of the United States, 2012).

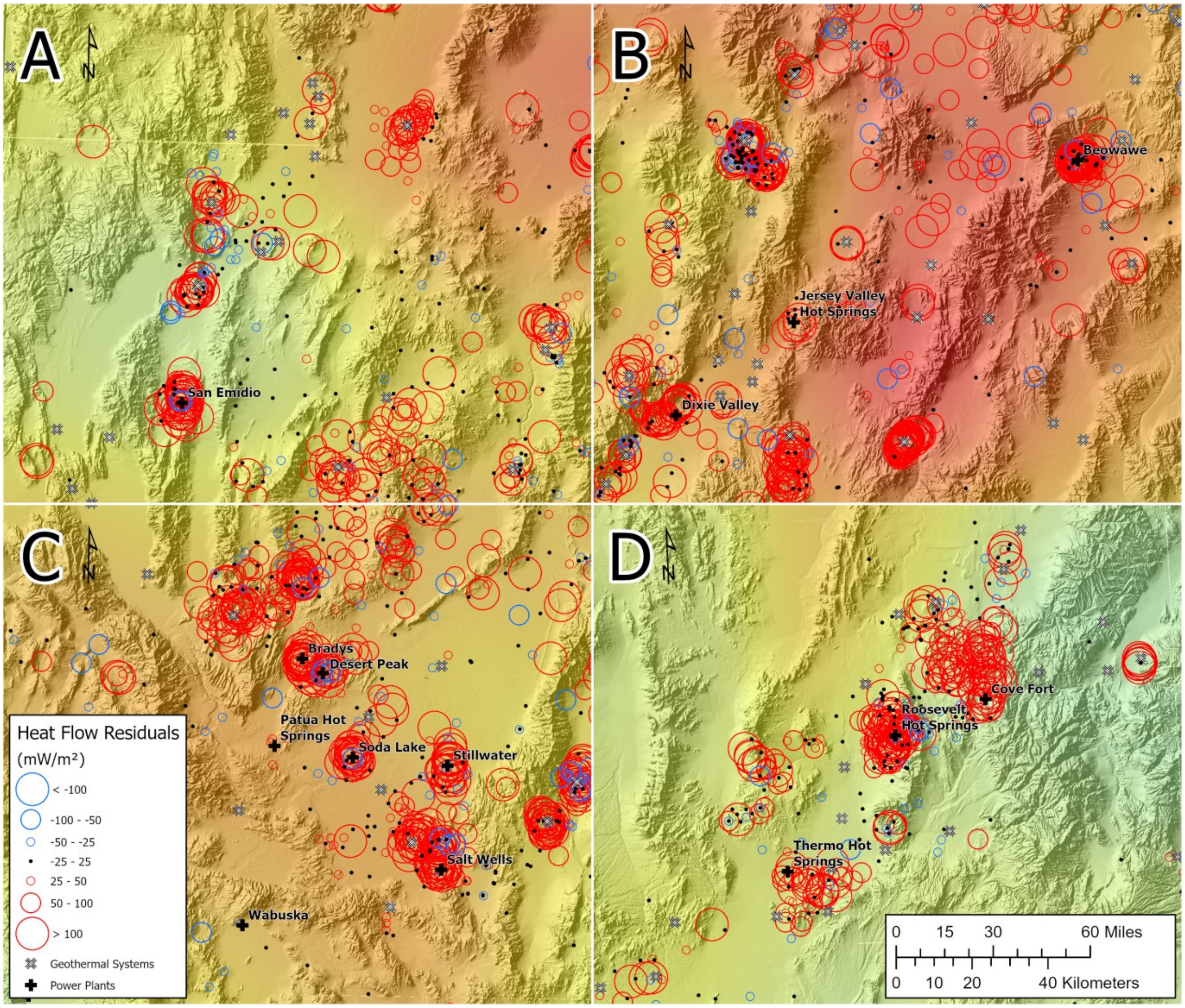

Figure 8: Heat flow residuals (mW/m²) from model de-emphasizing low-quality thermal gradient wells in example areas of geothermal interest, extents indicated by boxes shown in Figure 1 (DeAngelo et al., 2022). Black dots represent wells that have low residuals and are therefore likely to reflect background conductive conditions. Hollow circles represent heat flow wells with lower (blue) or higher (red) heat flow measurements than is estimated as background conductive heat flow; the hollow circles increase in size with increased magnitude of the residual. Geothermal systems and power plants (i.e., the compilation of mapped geothermal features and operating power plants from Faulds et al., 2021) show correlations between residuals and a range of known geothermal features. Hillshade derived from USGS National Atlas (National Atlas of the United States, 2012).

4. DISCUSSION

4.1 Separating Conductive and Convective Influences

The modeling strategies summarized in Section 3 were used to identify which geothermal wells were likely to reflect background conductive conditions and which wells were not, either due to convective influence (hydrothermal or hydrologic) or due to errors or uncertainties in the well data. The central tool in this effort was the LOESS algorithm (Cleveland et al., 1992; LOESS, 2022), used to estimate trends and calculate the local average conductive heat flow for every well and every grid cell. But the nature of the data made robust estimation of conductive heat flow impossible to do without devising solutions to the problems arising from having a noisy dataset with many errors and uncertainties, that was geographically clustered, and that contained many large outliers that are heavily influenced by convection.

The large outliers in the dataset (convective geothermal wells) probably posed the greatest challenge. This was overcome by implementing an iterative approach that assigned lower weights in each successive iteration to wells that departed further from the local and regional trends in estimated conductive heat flow. Iterative weights were assigned using a custom function that did not penalize measurements with small residuals, but that ensured that very large residuals had a very small effect on the resulting estimates of background conductive heat flow (Equation 1, Figure 3). This approach allowed for low-weighted wells to still have influence if there were no other wells nearby, but to impart very little influence when other wells with higher weights existed nearby. By reducing the weight of any high-residual well, the following iteration estimated heat flow for the well and surrounding area that is supported by hundreds of wells representative of regional trends. Iterations ceased when changes to residuals became smaller than 0.01 mW/m². This approach resulted in a model that effectively removed the influence of measurements representing strong convective influence, resulting in trend maps with unbiased fit to measurements that likely reflects conductive conditions. Unbiased fit was validated by 1) observing that residuals showed a symmetric distribution centered near 0 mW/m² (Figure 4), 2) observing that, even in areas with many convectively influenced wells, there were many interspersed and nearby low-residual wells (i.e., conductive wells shown as black dots in Figure 8 are interspersed among high-residual wells). The resulting background conductive heat flow maps honor previous observations, including: a) that the resulting heat flow surface ranged within expected values for the Great Basin region (~50 - 100 mW/m²), averaging 79.4 mW/m² with a standard deviation of 9.3 mW/m² which is consistent with anticipated background conductive heat flow of active tectonic areas (70-80 mW/m²; Pollack et al., 1993), and b) that major known features are replicated, such as the Battle Mountain High (lobe of high heat flow seen in north-central Nevada in Figures 5 and 6) and Eureka Low (lower values southeast of the Battle Mountain High) emerged from the process (Figures 5 & 6). Another region of high estimated regional heat flow was predicted to the east of the Battle Mountain High and south of the Snake River Plain; this region did not have very many wells, but the few wells that did exist generally agreed with the predicted values, so there is lower confidence in the predictions of this region. An additional strategy that de-weighted wells believed to have low-quality thermal gradient information further helped to remove the influence of data that were not likely to reflect actual background conductive heat flow. Wells with low-quality thermal gradient information were de-weighted in the model that was ultimately judged to be most useful (Table 1, Figures 2A & 5). This preferred model ended up assigning lower weights (Table 1) to wells that did not penetrate the Snake River Plain aquifer and were very likely reflecting cold-water transport above the conductive section beneath the aquifer. By de-weighting these hydrologically influenced wells that reflected conditions within the Snake River Plain aquifer, this preferred model seems more likely to reflect actual conditions of background conductive heat flow in and around the Snake River Plain (Figures 5, 7A).

Another major challenge had to do with modeling artifacts that were being generated near densely sampled areas. The LOESS algorithm uses a fixed fraction of data as controlled by the span parameter, which we have converted to a corresponding fixed number of wells to make predictions for each well and grid cell. A larger search radius is needed to reach a fixed number of wells in sparsely sampled areas and a smaller radius is needed in places with densely sampled wells. In very densely sampled areas, the small search radius resulted in trend surfaces that were representative of local variations or modeling artifacts, not regional trends. A strategy was therefore developed to emphasize wells representative of conductive conditions by removing wells from densely sampled areas that likely do not reflect conductive conditions. Wells had to meet three criteria: falling in a densely sampled area, not being labeled with the highest quality codes for thermal gradient and having a heat flow value far from the expected local trend when considering data from nearby regions. To determine to what degree a well was in a densely sampled area, declustering weights (Pyrcz et al., 2021) were calculated for each well. Wells with declustering weights below 1.5 were identified for possible removal from the interpolation from a sufficiently dense area; with this value being chosen by looking at a histogram of declustering weights and noting that there was a peak of low values in the distribution of weights that corresponds to common spacing of wells in locations where large amounts of geothermal exploration and development have occurred. However, wells with declustering weight <1.5 were never removed if they had either an ‘A’ or ‘B’ quality code (reflecting thermal gradient quality; SMU, 2021) because it was less likely for these wells to contain errors. Finally, all other wells with declustering weight <1.5 were removed when measured values were identified as being substantially different from nearby wells that were similar to background conditions estimated by regional trends in conductive heat flow. To estimate regional trends, an overly smooth model was generated using a large number of points (final value selected to be 800 points). This trend surface represents regional variation effectively to identify wells most representative of likely conductive conditions under densely sampled areas. A ‘substantial’ variation used for the purpose of removing convectively influenced wells was selected to correspond to a residual of ± 15 mW/m² because it is 20% of 75 mW/m², the approximate regional average of active tectonic areas (Pollack et al., 1993) and it has been previously estimated that high-quality wells (quality code = ‘A’ or ‘B’) can have errors up to 20% (Richards, 2013).

4.2 Residual Values are Important and Useful

A residual value was calculated for each well examined in the analysis. The residual value is a numeric measure of the departure of each heat flow measurement from estimated background conductive heat flow conditions, and therefore shows measurement errors, estimations errors, and convective influence. Known geothermal areas and areas around power plants contain many wells with very high residuals in this analysis (Figure 8) and are representative of large amounts of convective heat transport assuming measurement and interpolation errors are modest. Having a scalar residual value assigned to each well is valuable because it allows quantification of the convective influence from hydrothermal or hydrologic influences, and quantification of error in measurements or uncertainty in estimates of background conductive heat flow.

Assuming small residuals are essentially conductively dominated and large residuals have large convective components, patterns in residuals provide insight into physical processes related to the existence of permeability and hydrothermal circulation. Having a quantitative measure of this departure can possibly allow for these wells to be used as training data in data-driven geothermal energy assessments in a regression analysis where training data are not merely viewed as being positive or negative (classification-based), but as having a degree of being hydrothermally influenced. Residual values may also be important for other Earth science applications by identifying distinct upflow and downflow zones as identified by positive and negative residuals, respectively. Further, the residuals might be useful in delineating the boundaries of hydrothermal areas, although limited drilling data limit the ability to clearly delineate boundaries of hydrothermally influenced areas.

4.3 Measurement Confidence Weights Affect Resulting Heat Flow Maps and Residuals Estimates

The three alternate conductive heat flow maps presented herein (Figs 5 and 6) generally agree well, due to the use of large amounts of data, but there are a few key differences (Figure 7) related to physical processes that are represented by the confidence weights. The preferred model that assigned lower weights to wells with poor-quality thermal gradient data mainly shows discrepancies in and around the Snake River Plain by lowering the weight of the many measurements that are strongly influenced by advective transport of heat by the regional aquifer system. The major differences resulting from thermal conductivity estimate confidence weights (Figures 6B & 7B) were not similarly due to physical conditions; this model had systematic variations in confidence in densely sampled parts of the study area.

4.4 Considerations for Improvements to the Trend Analysis

Improvements to the dataset and analysis could seek to generate more accurate estimates and allow for the possibility of more localized modeling of variation in some areas.

- The LOESS algorithm was useful for its ability to generate local averages and trends, but it was limited by its need to have a fixed number of points in each calculation. Using a different algorithm or modifying LOESS to calculate local averages could prevent large differences in search radii being applied during modeling.
- Additionally, it may be possible to supplement the geothermal well data used in this analysis with other kinds of data, perhaps other well data, or perhaps proxy information such as temperatures derived from geochemistry, or alternate ways of estimating subsurface heat conditions such as estimates of the depth to the Curie isotherm (the depth at which rocks lose their magnetic properties).
- Finally, the heat flow data were very well curated by SMU, but the database still contained an unknown number of errors and uncertainties that surely propagated throughout the modeling. Any improvement to the accuracy of the heat flow database could make for a better final product. This, however, would be a laborious, manual task involving the examination of thousands of individual well records.

REFERENCES

Cleveland, W. S., Grosse, E., Shyu, W. M, 1992, Local regression models. Chapter 8 of Statistical Models in S eds J.M. Chambers and T.J. Hastie, Wadsworth & Brooks/Cole.

DeAngelo, J., Burns, E.R., Gentry, E., Batir, J.F., Lindsey, C.R., Mordensky, S.P., 2022, Heat flow maps and supporting data for the Great Basin, USA: U.S. Geological Survey data release, https://doi.org/10.5066/P9BZPVUC.

Faulds, J.E., Coolbaugh, M.F., Hinz, N.H., 2021, Inventory of structural settings for active geothermal systems and late Miocene (~8 Ma) to Quaternary epithermal mineral deposits in the Basin and Range province of Nevada: Nevada Bureau of Mines and Geology Report 58, 27 p., 3 plates, scale 1:2,500,000.

LOESS, 2022: r-loess, 2022: https://www.rdocumentation.org/search?q=loess.

National Atlas of the United States, 2012, 100-Meter Resolution Elevation of the Conterminous United States. National Atlas of the United States. Available at: http://purl.stanford.edu/zz186ss2071.

Pollack, H.N., Hurter, S.J., and Johnson, J.R. Heat flow from the Earth's interior: Analysis of the global data set: Reviews of Geophysics, 31, (1993), 267–80.

Pyrcz, M., Jo, H., Kupenko, A., Liu, W., Gigliotti, A. E., Salomaki, T., & Javier, S. (2021). GeostatsPy: Geostatistical Library in Python (Version 1.0.0) [Computer software]. https://doi.org/10.5281/zenodo.

Richards, Maria. Developing Geothermal Energy Resources, Mapping the Data. United States: N. p., 2013. Web.

Richards, M., Blackwell, D., Williams, M., Frone, Z., Dingwall, R., Batir, J., Chickering, C., (2012). Proposed reliability code for heat flow sites. Transactions, 36, 211-218.

Sass, J. H., S.S. Priest, A.H. Lachenbruch, S.P. Galanis, Jr., T.H. Moses, Jr., J.P. Kennelly, Jr., R.J. Munroe, E.P. Smith, F.V. Grubb, R.H. Husk, Jr., and C.W. Mase, 2005, Summary of supporting data for USGS regional heat flow studies of the Great Basin, 1970-1990, USGS Open file Report, 2005-1207.

SMU Regional Heat Flow Database, retrieved from http://geothermal.smu.edu on March 29, 2021.

U.S. Geological Survey, 2019, 3D Elevation Program 1-Meter Resolution Digital Elevation Model, https://www.usgs.gov/the-national-map-data-delivery.

University of Nevada, Reno. (2022). INGENIOUS Thermal Conductivity Measurement Source Categorization [data set]. Retrieved from https://gdr.openei.org/submissions/1390.